United States Department of Agriculture | **Natural Resources Conservation Service** | **11 Campus Boulevard Suite 200 Newtown Square, PA 19073**

Subject: SOI – Geophysical Assistance **Date:** 30 August 2002

To: Thomas E. Jewett
State Conservationist
USDA-NRCS,
220 East Rosser Avenue
P.O. Box 1458
Bismarck, ND 58502-1458

PURPOSE:
To evaluate the suitability of ground-penetrating radar (GPR) and electromagnetic induction (EMI) to determine depths to finer-textured materials and the water table in areas of coarse textured soils on the Souris and Sheyenne deltas of North Dakota.

PARTICIPANTS:
Joseph Brennan, Soil Scientist, USDA-NRCS, Devils Lake, ND
Jim Doolittle, Research Soil Scientist, USDA-NRCS, Newtown Square, PA
Lawrence E. Edland, Soil Data Quality Specialist, USDA-NRCS, Bismarck, ND
Cornelius J. Heidt, Soil Data Quality Specialist, USDA-NRCS, Bismarck, ND
David Hopkins, Associate Professor, Soils Department, NDSU, Fargo, ND
Earnest L. Jensen, MLRA Coordinator, USDA-NRCS, Devils Lake, ND
Robert H. Lisante, Area Resource Soil Scientist, USDA-NRCS, Devils Lake, ND
Michael G. Ulmer, Soil Data Quality Specialist, USDA-NRCS, Bismarck, ND

ACTIVITIES:
All field activities were completed during the period of 29 July to 2 August 2002.

RESULTS:

1. Because of the dominance of medium textured Mollisols formed in calcareous glacial drift with relatively high amounts of 2:1 expanding lattice clays, and the widespread occurrence of saline and sodic soils, North Dakota is considered generally unfavorable for the use of GPR. However, much of the southern half of the Souris Plain in McHenry and Pierce Counties and the Sheyenne Delta in Ransom County is covered by wind blown sand. These deposits are part of large deltas that formed where the ancestral Souris River entered glacial Lake Souris and the ancestral Sheyenne River entered Lake Agassiz. The sandy sediments that blanket this area appears suited to GPR. In these sandy sediments, depth of penetration appears limited principally by conductive groundwater or layers of medium textured materials (till or lacustrine substratum phases). Strong and significant correlations were found to exist between measured and interpreted depths to 2C horizons composed of finer-textured materials. In areas of Hecla and Maddock soils, GPR can be used to determine depths to finer-textured materials and to improve map unit concepts and interpretations.

2. Soil depth concepts have changed with time. Many areas of Hecla and Maddock soils were conceptualized at the time of mapping as having a deep (> 40 inches) soil depth class. Present concepts have moved the Hecla and Maddock soils into the very deep (>60 inches) soil depth class. GPR and EMI can be rapidly and effectively used in areas of Hecla and Maddock soils to obtain field data and to improve map unit concepts and interpretations.

3. With GPR, depths of penetration exceeded 3 m in areas of very deep moderately well to excessively drained sandy soils. However, in most medium textured soils with an active or superactive activity class, rates of

signal attenuation are exceptionally high and observation depths are restricted to depths of less than 50 cm. In areas of saline and sodic soils, penetration is restricted to the surface layers (<0.25 m).

4. A water table study beneath a low dune in the Sheyenne National Grassland demonstrated the rapid acquisition speed and reasonable accuracy of GPR. Being rapid, high-resolution radar imaging provides a practical, cost-effective, and effective method for mapping the water table in areas of coarse textured soils. Three-dimensional diagrams of the water table have the potential to greatly improve our knowledge of intricate local ground water patterns and recharge discharge processes.

5. EMI provide reasonably accurate predictions of the depths to medium textured 2C horizons in areas of Hecla and Maddock soils. Negative correlations (r = -0.74 to –0.78; 0.001 level) were obtained between depths to medium textured materials and EMI responses. The higher apparent conductivity at greater soil depths was in agreement with a conceptual model and was attributed to the presences of the medium-textured till or lacustrine deposits at lower soil depths.

6. Changes in EMI systems are rapidly evolving. With data loggers, surveys can be completed in the continuous mode and provide a large number of observations and more complete coverage of sites. Measurements from EMI instruments can be geo-referenced with GPS data eliminating the need for grids and providing the soil scientist with greater autonomy and mobility while eliminating the often-excessive time that is required to construct grids across units of management.

7. Field protocol needs to be developed to integrate these techniques with soil transect work. I will gladly avail myself to working with the Northern Great Plains Soil Survey Region (MO7) staff in developing field procedures for the use of EMI in North Dakota.

It was my pleasure to work in North Dakota and with members of your fine staff.

With kind regards,

James A. Doolittle
Research Soil Scientist

cc:
R. Ahrens, Director, USDA-USDA, National Soil Survey Center, Federal Building, Room 152,100 Centennial Mall North, Lincoln, NE 68508-3866
D. Hopkins, Assistant Professor, Soil Science Department, Bolley Drive, 233 Walster Hall, PO Box 5638, NDSU, Fargo, ND 58105
B. Hudson, Director of Soils Survey Division, USDA-NRCS, Room 4250 South Building, 14th & Independence Ave. SW, Washington, DC 20250
C. Olson, National Leader for Soil Investigations, USDA-USDA, National Soil Survey Center, Federal Building, Room 152, 100 Centennial Mall North, Lincoln, NE 68508-3866
W. Tuttle, Soil Scientist (Geophysical), USDA-NRCS-NSSC, P.O. Box 974, Federal Building, Room 206, 207 West Main Street, Wilkesboro, NC 28697
M. Ulmer, Soil Data Quality Specialist, USDA-NRCS, 220 East Rosser Ave., PO Box 1458, Bismarck, ND 58502-1458

MATERIALS AND METHODS

The radar unit is the Subsurface Interface Radar (SIR) System-2000, manufactured by Geophysical Survey Systems, Inc.[1] Morey (1974) and Doolittle (1987) discuss the use and operation of GPR. The SIR System-2000 consists of a digital control unit (DC-2000) with keypad, VGA video screen, and connector panel. A 12-volt battery powered the system. This unit is backpack portable and, with an antenna, requires two people to operate. The 200 MHz and 400 MHz antennas were used in this study.

The RADAN NT (version 2.0) software program was used to process the radar profiles (Geophysical Survey Systems, Inc, 2001a).[1] Processing included color transformation, marker editing, distance normalization, and range gain adjustments.

Geonics Limited manufactures the EM38DD meter.[1] Geonics Limited (2000) describes the principles of operation for this meter. The depth of penetration is "geometry limited" and is dependent upon the intercoil spacing, coil geometry, and frequency. The EM38DD operates at a frequency of 14,600 Hz. It has effective penetration depths of about 0.75 and 1.5 m in the horizontal and vertical dipole orientations, respectively (Geonics Limited, 2000). The EM38DD meter consists of two EM38 meters bolted together and electronically coupled. One unit acts as a master unit (meter that is positioned in the vertical dipole orientation and having both transmitter and receiver activated) and one unit acts as a slave unit (meter that is positioned in the horizontal dipole orientation with only the receiver switched on). The Geonics EM38Dpro Data Logging System was used to record and store both EMI and GPS data. [1] The logging system consists of an EM38DD meter, Allegro field computer, Trimble AG114 GPS receiver, backpack and frame for GPS, and associated cables. With the logging system, the EM38DD meter is keypad operated and measurements can either be automatically or manually triggered.

The GEM300 multifrequency sensor is manufactured by Geophysical Survey Systems, Inc. [1] Won and others (1996) describe the use and operation of this sensor. This sensor is configured to simultaneously measure up to 16 frequencies between 330 and 20,000 Hz with a fixed coil separation. With the GEM300 sensor, the penetration depth is considered "skin depth limited" rather than "geometry limited." The skin-depth represents the maximum depth of penetration and is frequency and soil dependent: low frequency signals travel farther through conductive mediums than high frequency signals. Theoretical penetration depths of the GEM300 sensor are dependent upon the bulk conductivity of the profiled earthen material(s) and the operating frequencies. Multifrequency sounding with the GEM300 theoretically allows multiple depths to be profiled with one pass of the sensor. The sensor is keypad operated and measurements can either be automatically or manually triggered. Unlike the EM38DD meter, simultaneous measurements of apparent conductivity in both dipole orientations are not possible with the GEM300 sensor; the sensor must be rotated to measure both dipole orientations.

To help summarize the results of this study, the SURFER for Windows (version 8.0) program, developed by Golden Software, Inc., [1] was used to construct two- and three-dimensional simulations[1]. Grids were created using kriging methods with an octant search.

GPR:

Calibration of GPR:

Ground-penetrating radar is a time scaled system. This geophysical tool measures the time it takes electromagnetic energy to travel from an antenna to an interface (i.e., soil horizon, water table, stratigraphic layer) and back. To convert travel time to depth requires knowledge of the velocity of pulse propagation. Several methods are available to determine the velocity of propagation. These methods include use of table values, common midpoint calibration, and calibration over a target of known depth. The last method is considered the most direct and accurate method to estimate propagation velocity. The procedure involves measuring the two-way travel time to a reflector of known depth on a radar profile and calculating the propagation velocity by the following equation (after Morey, 1974):

$$V = 2D/T \qquad [1]$$

[1] Manufacturer's names are provided for specific information; use does not constitute endorsement.

Equation [1] describes the relationship of the average propagation velocity (V) to the depth (D) and the two-way pulse travel time (T) to a reflector. Once the velocity of propagation is know, depths to interfaces are calculated by measuring the two-way travel time and using the following equation:

$$D = VT/2 \quad [2]$$

At sites in McHenry County, measured depths and two-way radar pulse travel times to well expressed, medium textured 2C horizons were used to estimate the velocity of propagation. In an area of Hecla loamy fine sand, 0 to 3 percent slopes (DesLauriers, 1990), the depth to the 2C horizon was measured at 12 observation points. Depths ranged from 1.35 to 1.75 m. The estimated average propagation velocity was 0.084 m/ns. The dielectric permittivity was about 12.6. The correlation (r) between measured and interpreted depths to the 2C horizon was 0.897. This relationship is shown in Chart 1. At the twelve observation points, the average difference between measured and interpreted depths to the 2C horizon was 0.09 m with a range of 0.0 to 0.21 m.

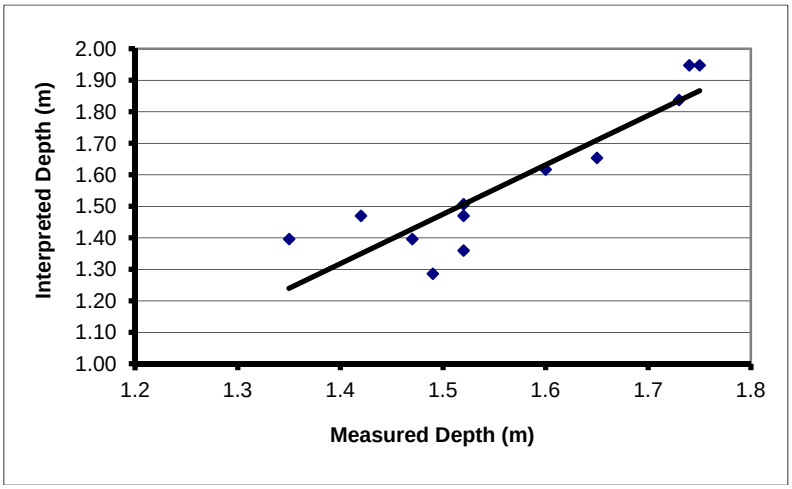

Chart 1. Relationship between measured and interpreted depths to a 2C horizon in an area of Hecla loamy fine sand, till substratum, 0 to 3 percent slopes (Hopkins and Sweeney, 1987), McHenry County.

In an area of Embden fine sandy loam, 0 to 3 percent slopes and Arvilla sandy loam, 0 to 6 percent slopes (DesLauriers, 1990) in McHenry County, measured depths and the two-way radar pulse travel times to a 2C horizon were used to estimate the velocity of propagation. Here, under drier soil conditions, the estimated velocity of propagation in the upper part of the soil profile was 0.113 m/ns. The dielectric permittivity was 6.9.

In an area of Barnes-Buse loam, 3 to 6 percent slopes and Lanona-Swenoda fine sandy loam, 2 to 6 percent slopes (Opdahl et al., 1990) in Barnes County, a metallic reflector was buried at a depth of 0.47 m. The estimated velocity of propagation through the upper part of the soil profile was 0.079 m/ns. The dielectric permittivity was 14.2.

In an area of Aylmer-Rosewood-Serden complex, 0 to 9 percent slopes (Edland, 1999) in the Sheyenne National Grassland, Ransom County, based on the measured depths and the two-way travel times to the water table at five wells, and equation [1], the velocity of propagation through the upper part of the Maddock and Hecla soil profiles was estimated to be about 0.196 m/ns. The dielectric permittivity was 2.3.

Chart 2 show the relationship between radar interpreted and measured depths to the water table at five monitoring wells. A strong (r = 0.98) and significant relationship (probability 0.001) exists between measured and interpreted depths. At the five wells, the average difference between measured and interpreted depths to the water table was 0.12 m with a range of 0.00 to 0.23 m.

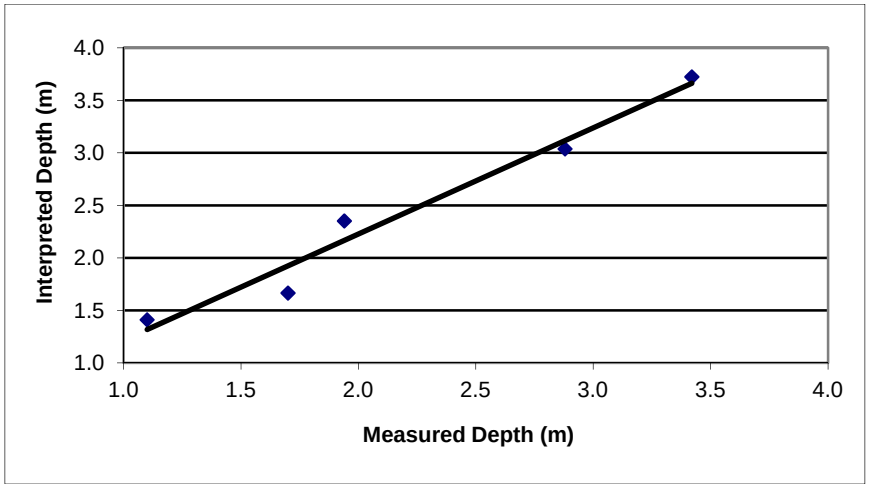

Chart 2. Relationship between measured and interpreted depths to the water table in an area of Aylmer-Rosewood-Serden complex, 0 to 9 percent slopes (Edland, 1999), Ransom County.

Background:
The performance of ground-penetrating radar (GPR) is dependent upon the electrical conductivity of soils. Soils having high electrical conductivity rapidly attenuate the radar energy, restrict penetration depths, and severely limit the effectiveness of GPR. Factors influencing the electrical conductivity of soils include the amount and type of salts in solution and the clay content. Because of their high adsorptive capacity for water and exchangeable cations, clays produce high attenuation losses. As a consequence, the penetration depth of GPR is inversely related to clay content. Doolittle and Collins (1998) noted that, depending on antenna frequency and the chemistry of the soil materials, penetration depths could range from 5 to 30 m in sandy (>85 % sand), 1 to 5 m in loamy (7 to 35 % clay), to less than 0.5 m in clayey (>35 % clay) soils. In addition, soils dominated by clay fractions having high amounts of smectite or vermiculite clay minerals have a higher CEC and are more attenuating to radar signal than soils dominated by non-expanding lattice clay minerals.

Electrical conductivity is a measure of the concentration of water-soluble salts in soils, and is directly related to the concentration of dissolved salts in solution, as well as the type of exchangeable cations and the degree of dissociation of the salts on soil particles (Soil Survey Staff, 1993). In semi-arid and arid regions, soluble salts of potassium and sodium and less soluble carbonates of calcium and magnesium are more likely to accumulate in the upper parts of the soil. These salts produce high attenuation losses that restrict the radar's penetration depths (Doolittle and Collins, 1995). Because of their high electrical conductivity, saline and sodic soils are unsuited to GPR. In these soils, penetration is restricted to the surface layers (<0.25 m).

In some areas (though especially in arid and semi-arid areas), high levels of calcium carbonate occur in soils. Though less attenuating than saline and sodic soils, soils with calcareous layers severely limits the penetration depths (0.5 to 1 m) (Grant and Schultz, 1994). These soils are considered poorly suited to GPR.

Because of the dominance of medium textured Mollisols that have formed in calcareous glacial drift with relatively high amounts of 2:1 expanding lattice clays, and the widespread occurrence of saline and sodic soils, North Dakota is considered generally unfavorable for the use of GPR. However, in a recently published map showing the suitability of soils for ground-penetrating radar, two conspicuous areas with high potential for GPR were identified in North Dakota: the Souris and Sheyenne deltas (Doolittle et al., 2002). According to this map, these areas are dominated by noncalcareous, coarse-textured soils that are well suited to GPR. Objectives of this investigation were to evaluate the accuracy of this map and to assess the suitability of soils to GPR in these two deltas.

Interpretations:
McHenry County:
A GPR survey was conducted in an area mapped as Hecla loamy fine sand, till substratum, 0 to 3 percent slopes (Hopkins and Sweeney, 1987) and Hecla loamy fine sand, 0 to 3 percent slopes (DesLauriers, 1990) located in southwest corner of Section 26, T 157 N, and R 79 W. The very deep, moderately well drained Hecla soil formed in sandy sediments on lake plains and glacial outwash plains. Hecla is a member of the sandy, mixed, frigid Oxyaquic

Hapludolls family. Include with Hecla soils in mapping are small areas of Maddock and Ulen soils. The very deep, well drained or somewhat excessively drained Maddock soil formed in fine sands deposited by wind or water. Maddock is a member of the sandy, mixed, frigid Entic Hapludolls family. The very deep, somewhat poorly drained Ulen soil formed in sandy glaciolacustrine deposits on glacial lake plains. Ulen is a member of the sandy, mixed, frigid Aeric Calciaquolls family.

An 84 m long traverse line was established across the soil delineation. Flags were inserted in the ground at about 7.5 m intervals and served as observation points. Pulling the radar antenna along the transect line completed the GPR survey. As the antenna was pulled passed each flag, the operator impressed a vertical line on the radar profile identifying the observation point. This provided 12 observation points. At each observation point soils were examined with a soil auger to the underlying, medium textured till or lacustrine layers. Based on auger observations, the traversed area contained about 58 percent Ulen soil and 42 percent Hecla soil.

Figure 1 is a portion of the radar profile from this site. The equally spaced (7.5-m), black, vertical marks at the top of the radar profile represent flagged observation points. This portion of the radar profile is 45 m long and contains 7 observation points. A depth scale (in meters) is provided along the left-hand margin of this figure. This scale is based on an average propagation velocity of 0.084 m/ns through the upper part of the soil profile. In this profile, the maximum observation depth is about 2.9 m.

In Figure 1 the interface that separates the sandy wind-blown sediments from the underlying medium-textured till is evident across the lower-center portion of the profile. Depths to the 2C horizon are easily and accurately estimated from the radar profiles. In this profile, the depth to this interface ranges from about 1.5 to 2 m. All soils are very deep to the 2C horizon. Ulen and Hecla soils dominated this portion of the radar traverse. Because of high rates of signal attenuation in the upper part of the 2C horizon, signal penetration is limited to this interface. The well-expressed, discontinuous, horizontal reflector in the upper part of the profile represents the calcic horizon of Ulen soil (best expressed in the left-hand portion of this profile, above the phrase “sandy sediments”).

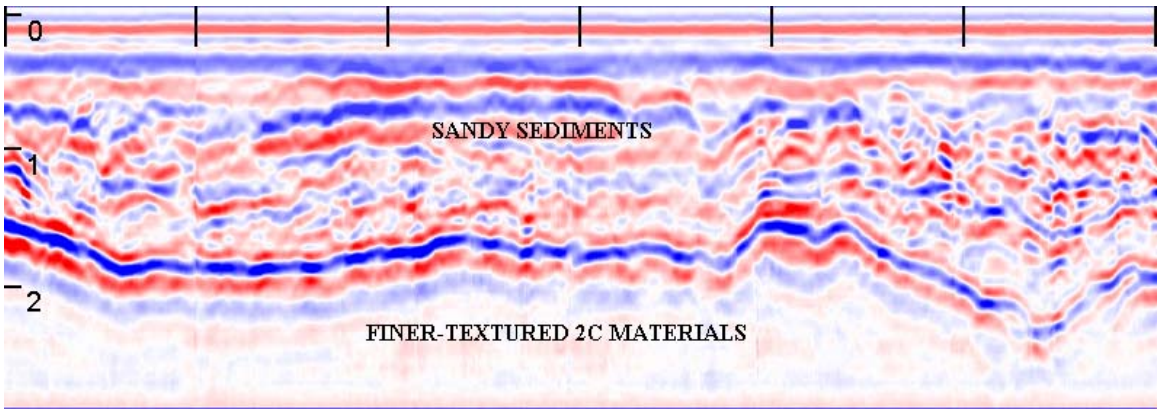

Figure 1. Representative GPR profile from an area of Hecla loamy fine sand, till substratum.

McHenry County Site #2:

The site is located in northwest corner of Section 23, T 157 N, and R 79 W. It is located in an area that has been mapped as Hecla loamy fine sand, 0 to 3 percent slopes and Maddock-Hecla loamy fine sand, 1 to 6 percent slopes (DesLauriers, 1990).

An approximate 91.5 m square grid was established across the survey area. Flags were inserted in the ground at 30.5 m intervals and served as observation points. Pulling the radar antenna along the transect line completed the GPR survey. As the antenna was pulled passed each flag, the operator impressed a vertical line on the radar profile identifying the observation point. This provided 16 observation points. At each observation point, soils were examined with a soil auger to the underlying, medium textured till or lacustrine layers.

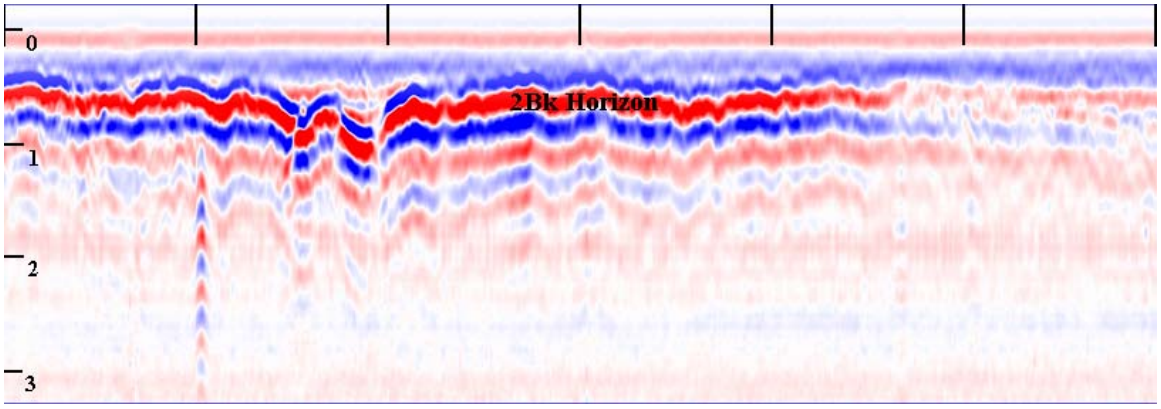

Figure 2. Representative GPR profile from an area of Swenoda and Towner soils.

At this site, the depth of radar penetration was restricted by a well-expressed 2Bk horizon. The 2Bk horizon had a very noticeable increase in not only carbonates but also clay content. Soils identified along the radar traverse included Towner and Swenoda. The very deep, well drained and moderately well drained Swenoda soil formed in loamy sediments underlain by silty and loamy sediments on uplands. Swenoda is a member of the coarse-loamy, mixed, superactive, frigid Pachic Hapludolls family. The very deep, well or moderately well drained Towner soil formed in wind and water deposited sands that are moderately deep over glacial till or lacustrine sediments. Towner is a member of the sandy over loamy, mixed, superactive, frigid Calcic Hapludolls family. In Figure 2, the well-expressed 2Bk horizon can be followed across the radar profile. Near the left-hand margin of this profile, the 2Bk horizon is at depths of less than 40 cm and is irresolvable from the surface pulse.

In Figure 2, based on a velocity of propagation of 0.11 m/ns through the upper part of the radar profile, a scanning time of 60 ns, and equation [1], the maximum depth of penetration is about 3.3 m. However, the maximum depth of observation is restricted by the 2Bk horizon and is generally less than 1 m in these medium textured, calcareous soils.

McHenry County Site #3:

The site is located in northwest corner of Section 36, T 157 N, and R 80 W. It is located in an area that has been mapped as Embden fine sandy loam, 0 to 3 percent slopes and Arvilla sandy loam, 0 to 6 percent slopes (DesLauriers, 1990); and Gardena loam, 0 to 3 percent slopes and Arvilla sandy loam, 0 to 6 percent slopes (Hopkins and Sweeney, 1987).

An approximate 97.5 m long traverse line was established across the survey area. Flags were inserted in the ground at 7.5 m intervals and served as observation points. Pulling the radar antenna along the transect line completed the GPR survey. As the antenna was pulled passed each flag, the operator impressed a vertical line on the radar profile identifying the observation point. This provided 14 observation points.

Figure 3 is a 67.5 m portion of the radar profile from this site. This profile extends from a low ridge (left-hand portion of profile) into a slough (right-hand portion of profile). Soils identified along this traverse include saline Balaton, Clontarf, Arvilla, and Marysland. The very deep, moderately well drained Balaton soil formed in calcareous loamy till. Balaton is a member of the fine-loamy, mixed, superactive, frigid Aquic Calciudolls family. The deep, moderately well drained Clontarf soil formed in loamy or loamy and sandy, glacio-lacustrine or outwash sediments. Clontarf is a member of the coarse-loamy, mixed, superactive, frigid Aquic Hapludolls family. The very deep, somewhat excessively drained Arvilla soil formed in moderately coarse textured glacial outwash and underlying sand and gravel. Arvilla is a member of the sandy, mixed, frigid Calcic Hapludolls family. The very deep, poorly and very poorly drained Marysland soil formed in a moderately deep loamy mantle over sandy or sandy-skeletal sediments. Marysland is a member of the fine-loamy over sandy or sandy-skeletal, mixed, superactive, frigid Typic Calciaquolls family.

In Figure 3, the equally spaced (7.5-m), black, vertical marks at the top of the radar profile represent flagged observation points. This portion of the profile contains 10 observation points. A depth scale (in meters) is provided along the left-hand margin of this figure. This scale is an approximation that is based on an average propagation velocity of 0.113 m/ns through the upper part of the Balaton soil profile. Based on this velocity and a scanning time of 80 ns, the maximum penetration depth is about 4.5 m.

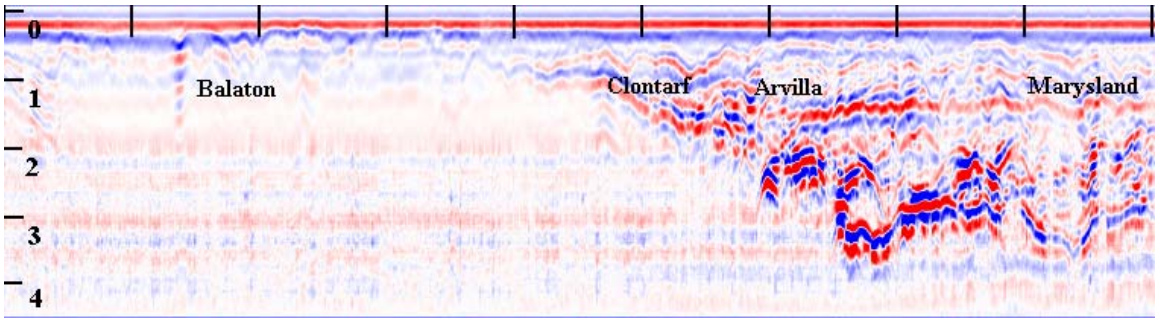

Figure 3. Representative GPR profile from an area mapped as Embden fine sandy loam, 0 to 3 percent slopes and Arvilla sandy loam, 0 to 6 percent slopes.

Profiling depths are severely restricted in areas of the saline, medium textured Balaton soil. The occurrence of saline soil conditions on this low ridge was a surprise to all participants. In areas of saline soils, depths of penetration were less than 0.25 m. As the radar descended the ridge and traverses areas of non-saline Clontarf and Arvilla soils, penetration depths increased. Reflectors in the upper part of these soils represent strata of coarse-textured materials. As reflected signals weaken near the right-hand margin of this profile, a gradual lateral increase in the clay content within the surface layers of Marysland soil is suspected. The highly irregular lower interface in the right hand portion of this profile defines the thickness of the overlying coarse textured deposits and the depth to the underlying, finer textured soil materials.

Barnes County:

Radar surveys were conducted in an area mapped as Barnes-Buse loam, 3 to 6 percent slopes and Lanona-Swenoda fine sandy loam, 2 to 6 percent slopes (Opdahl et al., 1990). The site was located in northwest corner of Section 8, T 139 N, and R 57 W. At the time of this investigation, the site was in wheat. Random traverses were conducted in included areas of Maddock soil and an unnamed Argiudolls with the 200 and 400 MHz antennas.

Figure 4 is a representative radar profile collected with the 200 MHz antenna in an area of Typic Argiudolls. The equally spaced (3-m), black, vertical marks at the top of the radar profile represent flagged observation points. The profile is about 21 m long and contains 8 observation points. A depth scale (in meters) is provided along the left-hand margin of this figure. This scale is based on an average propagation velocity of 0.079 m/ns through the upper part of the soil profile. Based on this velocity and a scanning time of 40 ns, the maximum penetration depth is about 1.6 m.

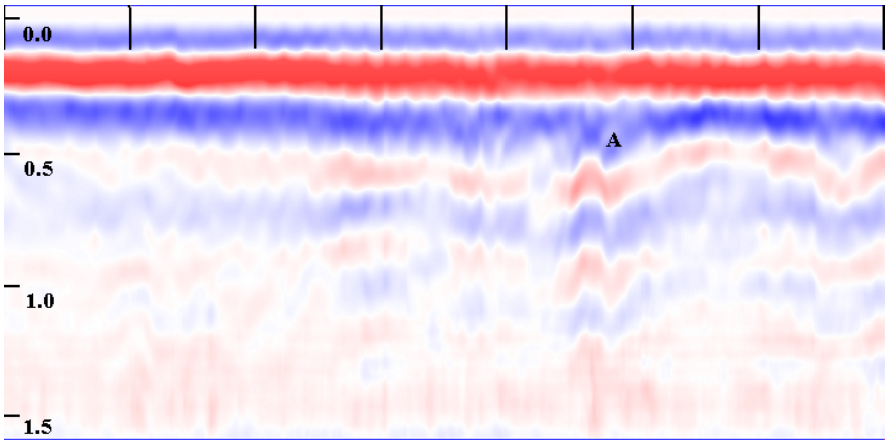

Figure 4. Representative GPR profile from an of Argiudolls in Barnes County.

In Figure 4, the point reflector that is labeled “A” represents a metallic reflector that was buried at a depth of 47 cm. This reflector is poorly expressed. It rests on the upper boundary of the argillic horizon. The wavy continuous line below “A” represents the upper boundary of the argillic horizon. In most medium-textured soils with an active or superactive activity class, rates of signal attenuation are exceptionally high and observation depths will be restricted to

depths of less than 50 cm. Figure 4 is an excellent example of the ineffectiveness of GPR in areas of fine-loamy or finer textured soils in North Dakota.

Water Table Study, Sheyenne National Grassland, Ransom County:
The depth and movement of groundwater through landscapes affect the physical and chemical properties and the morphology of soils (Richardson et al., 1992). Traditionally, information on the depth and movement of groundwater has been obtained by in-situ measurements at monitoring or observation wells. By recording water levels in these wells, depths to the water table are determined and potentiometric maps prepared. Although wells provide detailed information about soil and hydrologic conditions at specific points, lateral extension of this information has not been possible without an extensive and expensive system of monitoring wells. Typically, potentiometric maps are prepared from data collected from a few, widely spaced monitoring or observation wells. As a consequence, hydrologic conditions for the areas among and beyond the wells must be inferred. In relatively level landscapes containing homogeneous soil and geologic strata, hydrologic conditions are often relatively uniform and predictable. In areas of intricate and contrasting soil patterns, undulating topography, and non-homogeneous or anisotropic materials, depths to the water table and flow patterns are difficult to assess. Often in such areas, because of limited data, hydrologic models and maps are simplistic and susceptible to errors (Violette, 1987). Improved methods are needed to understand the depth, flow, and seasonal variations of the groundwater through complex landscapes.

New tools are available to chart water table depths and groundwater flow patterns. In areas of coarse-textured sediments, GPR can provide a continuous record of the water table, afford more comprehensive coverage of sites, and significantly reduce the number of wells. Ground-penetrating radar has been used to chart water table depths among observation wells and into nearby areas (Johnson, 1987; Bohling et al., 1989; Iivari and Doolittle, 1994, Doolittle et al., 2000). In addition, GPR has been used to provide data for hydrologic models (Violette, 1987; Taylor and Baker, 1988), define recharge and discharge areas (Johnson, 1987; Bohling et al., 1989), predict ground-water flow patterns (Steenhuis et al., 1990; Iivari and Doolittle, 1994; Doolittle et al., 2000), and delineate near-surface hydrologic conditions (Beres and Haeni, 1991). Data from GPR profiles have been used to construct three-dimensional computer simulations showing ground-water flow patterns in stratified, coarse-textured soils (Iivari and Doolittle, 1994, Doolittle et al., 2000).

Two-dimensional radar profiles have been used to identify and chart depths to the water table. However, a major constraint of two-dimensional radar profiling has been its inability to adequately resolve and disclose the often complex, three-dimensional geometries of the water table beneath complex and undulating landscapes. Comparisons of multiple, adjacent parallel radar traces are awkward and time-consuming tasks. Recent advancements in processing technologies have facilitated the manipulation of large sets data and the creation of three-dimensional radar images. These displays have provided unique, multiple viewpoints to analyze the subsurface.

Three-dimensional images provide multiple perspectives from which to view and analyze the subsurface. Junck and Jol (2000) noted that, with 3D images, “The internal stratigraphy and geometry of geomorphic environments can be interpreted in more detail than with widely spaced 2D transects, and reflection patterns can be compared with better spatial awareness.” By means of time-slices, 3D block, chair, or fence diagrams, three-dimensional images of the water table can be selected to better visualize and determine subsurface form and geometry. The objectives of this study were to see if three-dimensional displays of GPR data provide a more useful way to view and analyze the depth and geometry of the water table and evaluate flow patterns in a dunal landscape in North Dakota.

Study Area:
The dune selected for this investigation is in the Sheyenne National Grassland, Ransom County. The dune is located about 21 km east of Lisbon, in the NW 1/4 quarter of Section 7, T 134 N, R 54 W (about 550 meters south and 350 meters east of the NW corner of Section 7). The dune is in a delineated area of Aylmer-Rosewood-Serden complex, 0 to 9 percent slopes (Edland, 1999). The very deep, moderately well drained, Aylmer soil formed in wind worked sand on outwash plains and delta plains. A water table is seasonally within depths of about 0.5 to 1.0 m. Aylmer is a member of the mixed, frigid Aquic Udipsamments family. The very deep, poorly and very poorly drained Rosewood soil formed in calcareous sandy lacustrine sediments on glacial lake plains. Rosewood soil is on lower-lying concave slopes and has a water table that is seasonally within depths of about 0.2 to 0.5 m. Rosewood is a member of the sandy, mixed, frigid Typic Calciaquolls family. The very deep, excessively drained, Serden soil formed in wind

worked deposits. Serden soil is on higher-lying convex surfaces of dunes. Serden is a member of the mixed, frigid Typic Udipsamments family.

Field Procedures:
A 36 by 45 m grid was established across a small, low dune. The grid interval was 3 m. Survey flags were inserted in the ground at each grid intersection and served as observation or reference points. This procedure resulted in 208 equally spaced observation points. The origin of the grid was located in the southwest corner of the survey area. The elevation of each observation point was measured with a theodolite and stadia rod. Elevations were not tied to a benchmark; the lowest recorded surface point was chosen as an arbitrary 325 m datum. The measured relief was 2.93 m. The topography of the study site has been simulated in the left-hand plot of Figure 5. In this plot, the contour interval is 0.5 m. The orientation of the dune's long axis is northwest to southeast. The dune is bordered by depressions to the northwest, north, and southeast.

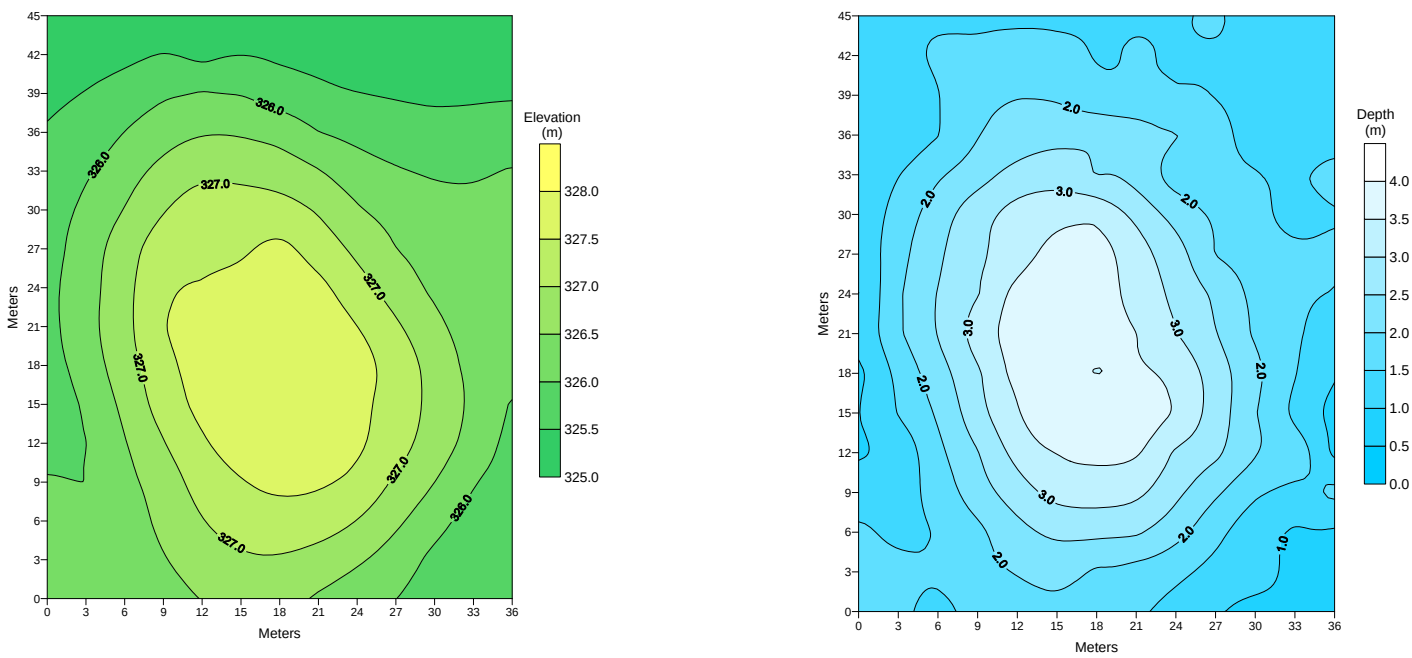

Figure 5. Two-dimensional contour plots of dune surface (left-hand plot) and the water table (right-hand plot). Sheyenne National Grassland, Ransom County. All units are in meters.

Survey procedures were modified to facilitate the construction of 3-D images and the interpretation of subsurface features. To construct three-dimensional displays, the imagery between adjoining radar profiles is interpolated. As a consequence, the quality and detail of a three-dimensional display will increase as the spacing between survey lines is decreased (Geophysical Survey Systems, Inc., 2001b). As a general rule, lines should be spaced so that the radar beams from adjacent lines overlap at the depth of interest. (Geophysical Survey Systems, Inc., 2001b). Generally these lines should be closely spaced (0.5 to 1 m apart). However, because of the size of dune and the lucid and consistent imagery from the water table interface, economy dictated a wider spacing of 3 m. Data were processed into a three-dimensional image through the 3D QuickDraw for RADAN Windows NT software developed by Geophysical Survey Systems, Inc. [2] Once processed, arbitrary cross-sections, insets, and time slices can be quickly viewed and extracted from the three-dimensional data set. The flexibility of three-dimensional visualizations can facilitate the interpretation of spatial relationships and the analysis of the water table. This imaging technique enables users to quickly view the subsurface from nearly any perspective.

GPR Surveys were conducted along 16 equally spaced (3 m), east-west trending grid lines. Each radar traverse was 36-m long. Pulling the 200 MHz antenna by hand along each of the sixteen lines completed the radar survey. Lines were sequentially profiled with the radar in a back and forth, snake line fashion. Along each line, as the antenna passed each

[2] Manufacturer's names are provided for specific information; use does not constitute endorsement.

observation point, a vertical mark was impressed on the radar profile. At each marked observation point on the radar profiles, the water table reflection was identified and the two-way travel time to this reflector was measured.

The depth to the water table was measured at four well and correlated with the radar imagery. Based on the measured depths and the two-way travel times to the water table at five wells, and equation [1], the velocity of propagation through the upper part of the soil profile was estimated to be about 0.196 m/ns. The dielectric permittivity was 2.3. Chart 2 shows the relationship between the measured depths and the two-way travel time to the water table at the five wells. A strong (r = 0.987) and significant positive relationship exists between travel time and depth to water table.

A scanning time of 60 nanoseconds was used in this investigation. Using a propagation velocity of 0.196 m/ns and equation [2], the difference between measured and interpreted depths to the water table at the five wells was 0.12 m with a range of 0.0 to 0.23 m. The interpreted depths to the water table have been simulated in the right-hand plot of Figure 5. This plot is base on interpretations made at 208 grid intersections or observation points. In this plot, the contour interval is 0.5 m. The plot of water table depths mimics the topography of the dune.

Radar Interpretations:

Figure 6 is the first radar profile obtained with the 200 MHz antenna within the grid. The equally spaced (3-m), black, vertical marks at the top of the radar profile represent flagged observation points. The profile is about 36 m long and contains 13 observation points. A depth scale (in meters) is provided along the left-hand margin of this figure. This scale is based on an average propagation velocity of 0.196 m/ns through the upper part of the soil profile. Based on this velocity and a scanning time of 60 ns, the maximum penetration depth is estimated to be about 5.9 m.

The water table provides an abrupt contrast in dielectric properties between the unsaturated sands above and the saturated sands below. As a consequence, the water table provides a continuous, high amplitude reflection that is easily identified and traced laterally across the radar profile.

In Figure 6, the soil surface, is portrayed as a level reflector. The water table appears undulating. However, the topography of the water table is the inverse of the topography of the soil surface: where the soil surface rises in elevation the water table appears to plunge to greater depth, and where the soil surface falls in elevation the water table appears to climb towards the surface. In Figure 7, the surface has been terrain corrected to improve the visual presentation. Through a process known as “surface normalization” elevations are assigned to each observation point and the image is corrected for changes in elevation. Surface normalization adjusts the vertical to remove topographic effects. Surface normalization results in the water table, appearing as a horizontal or near horizontal reflector.

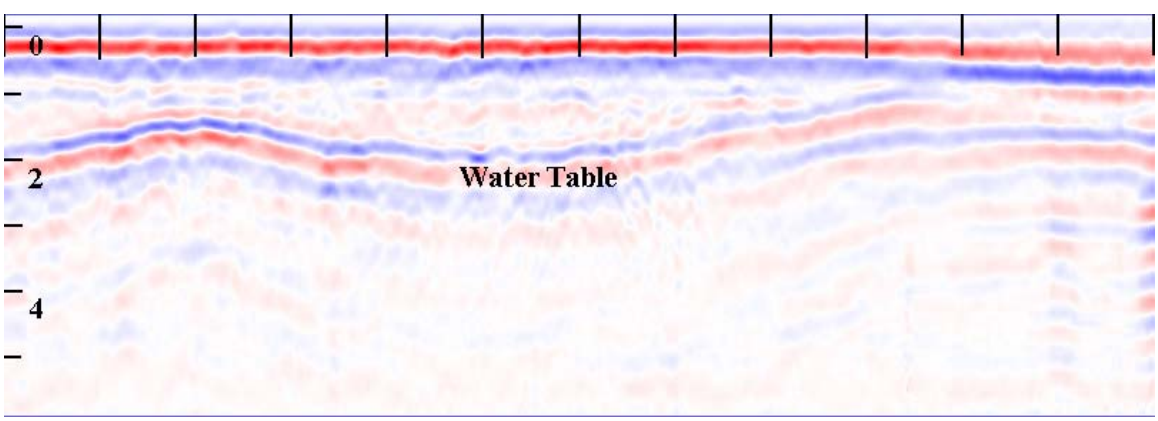

Figure 6. A typical radar profile across the dune showing the reflection from the water table. Sheyenne National Grassland, Ransom County. All units are in meters.

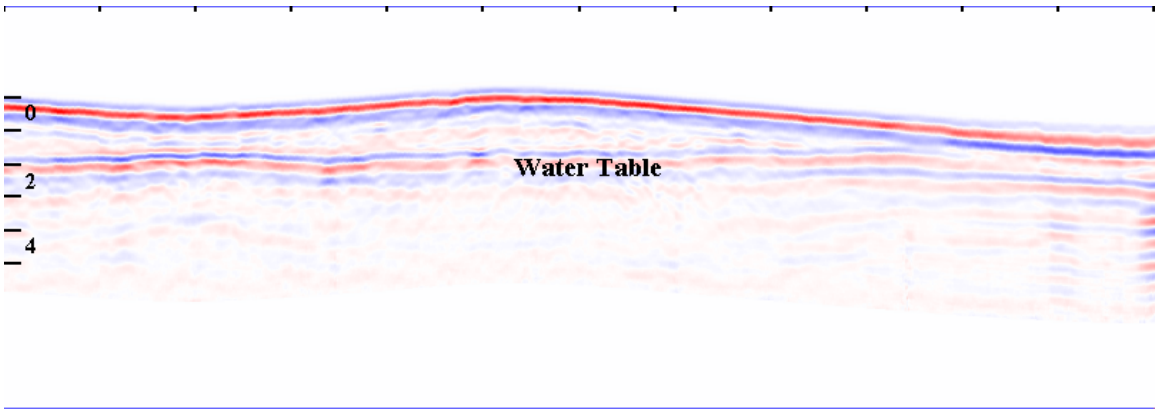

Figure 7. A radar profile that has had its vertical scale adjusted to account for changes in topography. Sheyenne National Grassland, Ransom County. All units are in meters

Software:
The 3D QuickDraw module for RADAN NT was used to construct and analyze three-dimensional displays of the radar data. This module permits the simultaneous viewing of multiple radar profiles from the survey area. With the 3D QuickDraw module, three-dimensional simulations of radar data can be rapidly created, displayed, and adjusted to observe subsurface features at different depths or from different perspectives.

A file was created from the sixteen radar profiles collected within the grid area. This file consists of the orderly succession of parallel radar profile lines that are processed together. A macro was created to further process this radar file. To create a three-dimensional display, radar profiles are appended to one another in order of increasing Y-coordinates. Simulations are created from this file having the X-axis parallel, and the Y-axis orthogonal to the radar survey lines.

3D Interpretations:
Figure 8 is a fence diagram showing the three dimensionality of the water table beneath the dune. In this figure, all units are in meters. The diagram shown in Figure 8 is composed of two intersecting lines. The orientation of the grid in Figure 8 is identical to the orientation of the grids shown in Figure 5. The origin is located in the southwest corner of the grid. In Figure 8, the water table is well expressed. The water table provides a continuous, high amplitude planar reflector that is easily identified and traced laterally in most visible areas of this diagram. However along the north-south line (line that is parallel with Y axis) the water table is partially obscured by several closely spaced and sub-parallel planar reflectors that represent stratigraphic layers within the dune. The water table appears slightly lower in the interior of the dune. The water table appears to ascend most noticeably beneath concave portions of lower side slopes.

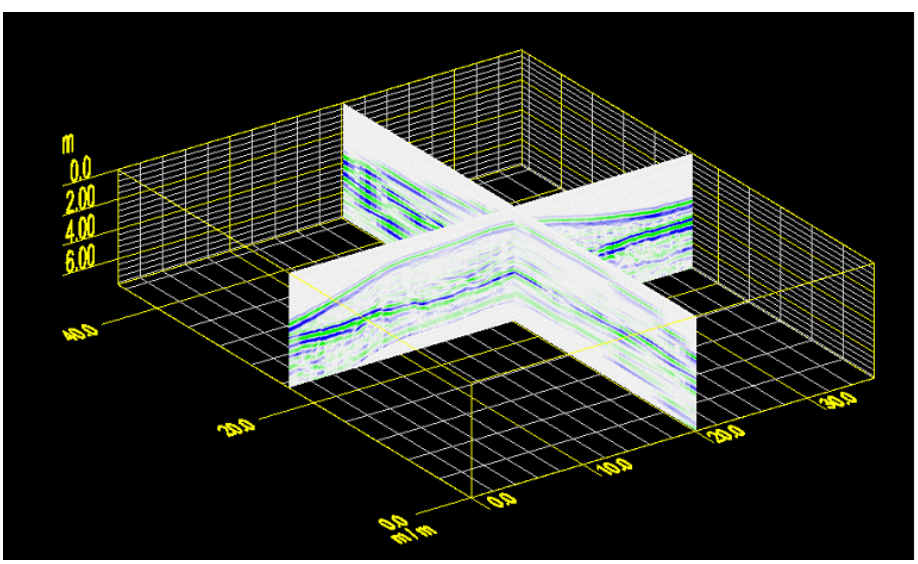

Figure 8. An X-Y fence diagram showing the water table in three dimensions.

Figure 9 is a fence diagram showing four lines that are parallel with the x-axis and extending across the grid in an east-west direction. All units are in meters. The orientation of this grid is identical to the orientation of the other grids. The origin is located in the southwest corner of the grid. In Figure 9, the water table is well expressed in all segments. Along the first three lines (lines Y = 0, 15, and 30 m) the water table appears to dip slightly below the dune. It is inferred from this diagram that the water is flowing from the margins of the dune into the dune's interior. The water table is difficult to identify on the northern-most line (line Y = 45 m,). Most portions of this line are within a wetland. Soils along this line were noticeably wetter and had thicker mats of vegetation. Strongly expressed, planar reflectors are more numerous in the upper part of this profile. As these interfaces parallel the soil surface and the water table, the identification of the water table is more problematic.

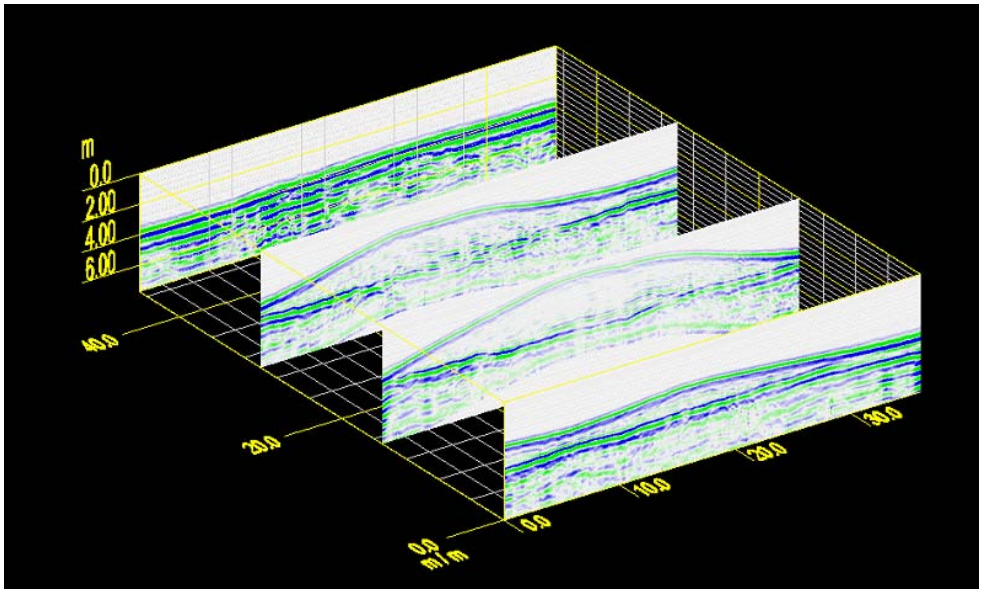

Figure 9. An X fence diagram showing the depth and geometry of the water table to the topography dune.

Figure 10 is a "chair" diagram that has been generated from the same radar data. The cube has the same orientation as the other diagrams. A sub-block has been removed from the cube along different X and Y axes coordinates. The 3D software allows the viewing of data from any angle and the analysis of reflector continuity through cutouts of the cube.

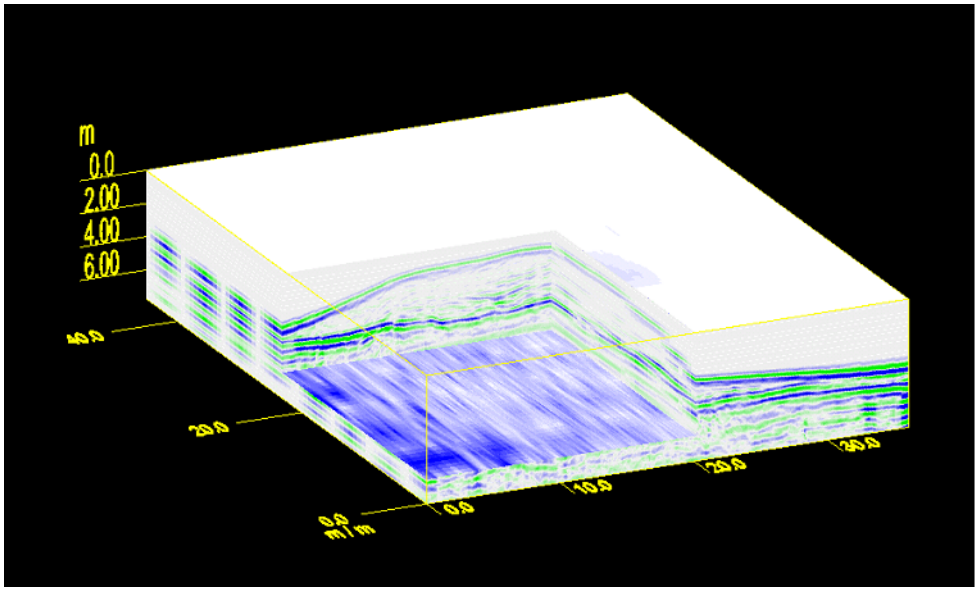

Figure 10. A 3D cube of the dune with deep inset into the feature.

This study demonstrated the rapid acquisition speed of data needed to construct three-dimensional simulations of radar profile. Being rapid, high-resolution radar imaging provides a practical, cost-effective, and effective method for mapping the water table in coarse textured soils. Three-dimensional diagrams of the water table have the potential to greatly improve our knowledge of intricate local ground water patterns and recharge discharge processes.

EMI:
Electromagnetic induction is a noninvasive geophysical tool that is used for high intensity surveys and detailed site assessments. Advantages of EMI are its portability, speed of operation, flexible observation depths, and moderate resolution of subsurface features. Results of EMI surveys are interpretable in the field. This geophysical method can provide in a relatively short time the large number of observations that are needed to comprehensively cover sites. Maps prepared from correctly interpreted EMI data provide the basis for characterizing site conditions, planning further investigations, and locating sampling or monitoring sites.

Electromagnetic induction uses electromagnetic energy to measure the apparent conductivity of earthen materials. Apparent conductivity is a weighted, average conductivity measurement for a column of earthen materials to a specific observation depth (Greenhouse and Slaine, 1983). Variations in apparent conductivity are caused by changes in the electrical conductivity of earthen materials. Electrical conductivity is influenced by the volumetric water content, phase of the soil water, temperature, type and concentration of ions in solution, and amount and type of clays in the soil matrix (McNeill, 1980). Apparent conductivity is principally a measure of the combined interaction of the soil's soluble salt content, clay content and mineralogy, and water content. The apparent conductivity of soils increases with increased soluble salts, clay, and water contents (Kachanoski et al., 1988; Rhoades et al., 1976). In any soil-landscape, variations in one or more of these factors may dominate the EMI response.

Though seldom diagnostic in itself, lateral and vertical variations in apparent conductivity have been used to infer changes in soils and soil properties. As EMI measurements integrate the bulk physical and chemical properties for a defined observation depth into a single value, responses can be associated with changes in soils and soil map units (Doolittle et al., 1996; Jaynes et al., 1993). For each soil, the inherent variability in physical and chemical properties, as well as temporal variations in soil water and temperature, will establish a unique and characteristic range of observable apparent conductivity values. Recently, EMI has been used as a soil-mapping tool to assist precision farming (Jaynes et al., 1993; Sudduth et al., 1995).

Electromagnetic induction is not suitable for use in all soil investigations. Generally, the use of EMI has been most successful in areas where subsurface properties are reasonably homogeneous, the effects of one property (e.g. clay, water, or salt content) dominates over the other properties, and variations in EMI response can be related to changes in the dominant property (Cook et al., 1992). Within a given geographic area, most similar soils should have comparable EMI responses. Dissimilar soils should have disparate EMI responses. However, the conductivities of some similar and dissimilar soils will overlap. This occurs where contrasts in EMI responses caused by differences in one property are offset by differences in another property. Some soil properties and soils can be inferred or predicted with EMI provided one is cognizant of changes in parent materials, topography, drainage, and vegetation.

The objectives of this study were to evaluate the potential of using EMI to map the depths to finer-textured materials in areas of coarse-textured soils.

Study Site:
The site is located on the Souris Delta in McHenry County. It is located in northwest corner of Section 23, T 157 N, and R 79 W. The study area had been mapped as Hecla loamy fine sand, 0 to 3 percent slopes and Maddock-Hecla loamy fine sand, 1 to 6 percent slopes (DesLauriers, 1990). At the time of the survey, soils were dry through.

Field Procedures:
A 91.5 m square grid was established across the survey area. Flags were inserted in the ground at 30.5 m intervals and served as observation points. This provided 16 observation points. At each observation point soils were examined with a soil auger and the depths to the underlying, medium textured till or lacustrine layers determined.

Multiple surveys were completed with the EM38DD meter and the GEM300 sensor. As measurements were obtained in both the horizontal and vertical dipole orientations and precise positioning of both instruments were required, EMI surveys were conducted in a station-to-station rather than a continuous mode. Apparent conductivity measurements

were recorded at each observation point with an EM38DD meter placed on the ground surface in both the horizontal and vertical dipole orientations. At each observation point, measurements were recorded with the GEM300 sensor at three different frequencies (6030, 9810, and 14790 Hz). Measurements were taken with the GEM300 sensor held at hip-height in both the horizontal and vertical dipole orientations.

Results:
Based on sixteen auger measurements, the depth to medium textured till or lacustrine deposits averaged 0.90 m with a range of 0.46 to 1.32. One-half of the observations had depths to a medium textured 2C horizon between 0.76 to 1.07 m. The medium textured deposits were shallow (< 0.5 m) at 6 percent, moderately deep (0.5 to 1.0 m) at 56 percent, and deep (1 to 1.5 m) at 38 percent of the observation points. The preponderance of shallow and moderately deep soils is not in accord with the soils and map units delineated within the study site. Measured depths to medium textured till or lacustrine deposits have been plotted in Figure 11. In general, depths to the 2C horizon were greater on higher-lying plane and convex surfaces. Depths to the 2C horizon were shallower on lower-lying concave surfaces.

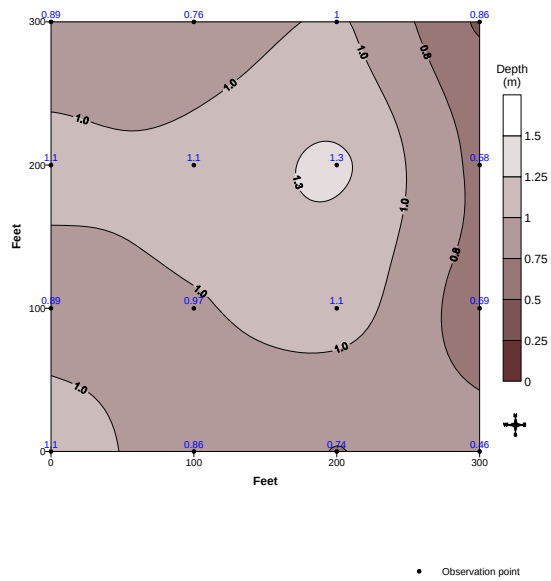

Figure 11. Depth to medium textured materials in an area of Hecla and Maddock soils.

Measurements obtained with the EM38DD meter are displayed in Table 1. In the horizontal dipole orientation, apparent conductivity averaged 13.8 mS/m and ranged from 7.0 to 29.8 mS/m. One-half of the observations had an apparent conductivity between 10.4 and 16.4 mS/m. In the vertical dipole orientation, apparent conductivity averaged 26.2 mS/m with a range of 14.2 to 52.2 mS/m. One-half of the observations had an apparent conductivity between 18.7 and 32.4 mS/m. Apparent conductivity increased and became more variable with increasing soil depth (vertical dipole measurements were greater than horizontal dipole measurements). The higher apparent conductivity at greater soil depths was in agreement with the conceptual model for this site and was attributed to the presences of the medium-textured till or lacustrine deposits at lower soil depths.

Measurements obtained with the GEM300 sensor are shown in Table 2. At each frequency, data obtained in the deeper-sensing vertical dipole orientation (V) were higher and more variable than data obtained in the shallower-sensing horizontal dipole orientation (H). With a frequency of 6030 Hz, apparent conductivity averaged 19.0 mS/m and ranged from 8.3 to 38.1 mS/m in the horizontal dipole orientation. In the vertical dipole orientation, apparent conductivity averaged 34.9 mS/m with a range of 15.6 to 69.9 mS/m. With a frequency of 9810 Hz, apparent conductivity averaged 18.2 mS/m and ranged from 6.9 to 37.2 mS/m in the horizontal dipole orientation. In the vertical dipole orientation, apparent conductivity averaged 35.4 mS/m with a range of 16.3 to 69.8 mS/m. With a frequency of 14790 Hz, apparent conductivity averaged 21.5 mS/m and ranged from 11.0 to 39.8 mS/m in the horizontal dipole orientation. In the vertical dipole orientation, apparent conductivity averaged 39.0 mS/m with a range of 19.0 to 73.4 mS/m.

Table 1. Measurements obtained with the EM38DD Meter

X	Y	Vertical	Horizontal
0	0	20.1	7.9
0	100	23.2	12.7
0	200	25.4	14.3
0	300	28.4	14.2
100	0	15.3	7.2
100	100	14.2	9.5
100	200	18.8	12.0
100	300	32.0	16.9
200	0	24.1	14.3
200	100	18.3	7.0
200	200	17.2	10.7
200	300	24.5	16.2
300	0	33.4	13.4
300	100	34.3	17.6
300	200	38.2	16.8
300	300	52.2	29.8

Table 2. Measurements obtained with the GEM300 sensor.

X	Y	6030V	6030H	9810V	9810H	14790V	14790H
0	0	23.9	12.2	24.9	12.0	29.0	15.6
0	100	29.9	15.8	29.7	15.3	33.5	18.3
0	200	28.1	15.9	29.0	17.0	33.0	18.2
0	300	31.6	18.8	32.7	17.2	36.3	21.9
100	0	20.1	9.7	20.7	8.9	23.6	13.0
100	100	15.6	8.3	16.3	6.9	19.0	11.0
100	200	19.2	11.6	20.1	9.4	23.8	13.5
100	300	41.6	22.6	42.0	21.6	45.6	25.4
200	0	29.4	16.2	29.9	15.2	33.1	17.9
200	100	21.6	11.7	21.5	8.9	25.5	14.0
200	200	26.0	13.3	26.2	15.9	29.9	16.5
200	300	36.9	19.3	37.4	18.6	40.2	20.6
300	0	46.7	26.1	48.0	26.1	52.2	29.1
300	100	58.1	31.0	58.2	29.7	62.2	32.9
300	200	60.0	32.7	60.7	31.3	64.4	36.1
300	300	69.9	38.1	69.8	37.2	73.4	39.8

Measurements of apparent conductivity collected with the GEM300 sensor, though comparable, were higher and more variable than those collected with the EM38DD meter. Differences in equipment calibration by the manufacturers are believed to explain the higher values of apparent conductivity recorded by the GEM300 sensor than by the EM38 meter. In addition, differences in the depth of penetration, volume of soil material measured, and resolution of each tool will affect measurements.

Figures 12 and 13 are two-dimensional plots of apparent conductivity collected at each observation point with the EM38DD meter and the GEM300 sensor, respectfully. In each plot the isoline interval is 5 mS/m. In Figure 13, each plot depicts measurements of apparent conductivity collected with the GEM300 sensor at a specified frequency in either the horizontal or vertical dipole orientation. Spatial patterns of apparent conductivity appearing in figures 12 and 13 are similar and generally correspond to the patterns of soil depths shown in Figure 11. Areas of higher apparent conductivity are associated with areas with shallower depths to medium textured materials. Areas of lower apparent conductivity are associated with areas with deeper depths to medium textured materials.

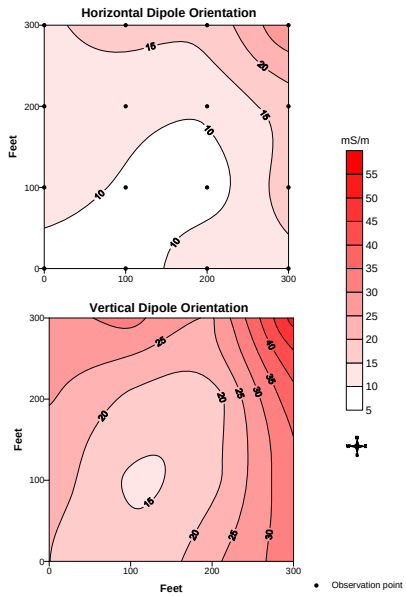

Figure 12. Apparent conductivity measured with the EM38DD meter in an area of Hecla and Maddock soils.

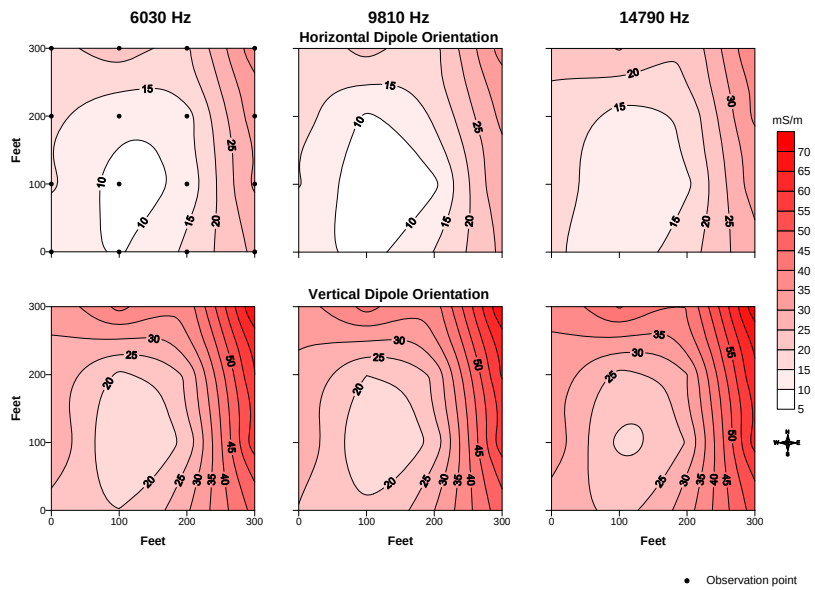

Figure 13. Apparent conductivity measured with the GEM300 sensor in an area of Hecla and Maddock soils.

Negative correlations (r = -0.74 to –0.78; 0.001 level) were obtained between depths to medium textured materials and EMI responses. This relationship conforms to the basic conceptual model of the site: the underlying medium-textured soil materials have higher clay, moisture, and soluble salt contents and is therefore more conductive than the overlying coarse-textured soil materials. Areas having greater depths to medium textured materials will have lower EMI responses. The highest correlations were between the depth to medium textured materials and EMI responses recorded with the GEM300 sensor at a frequency of 6030 Hz in the vertical dipole orientation and the EM38DD meter in the vertical dipole orientation.

Data collected with the GEM300 sensor and the EM38DD meter at the sixteen sampling points were used to develop the following predictive regression equations:

$$D = 1.2835 + (-0.01084 * 6030\text{Hz}) \quad [3]$$

$$D = 1.3714 + (-0.01779 * \text{EM38DD-V}) \quad [4]$$

Where "D" is depth to the 2C horizon, and "6030 Hz" is the apparent conductivity measured with the GEM300 sensor at a frequency of 6030 Hz in the vertical dipole orientation; and “EM38DD-V” is the apparent conductivity measured with the EM38DD meter in the vertical dipole orientation.

For the sixteen observation sites, using responses measured with the GEM300 sensor and predictive equation [2], the average difference between measured and predicted depth to the 2C horizon was 0.11 m with a range of 0.01 to 0.32m. For the sixteen observation sites, using responses measured with the EM38DD meter and predictive equation [3], the average difference between measured and predicted depth to the 2C horizon was 0.11 m with a range of 0.01 to 0.25m.

Based on sixteen soil auger measurements, the depths to the 2C horizon were shallow at 6 percent, moderately deep at 56 percent, and deep at 38 percent of the observation points. Based on sixteen measurements made with the GEM300 sensor operating at a frequency of 6030 Hz in the vertical dipole orientation and equation [3], the depths to the 2C horizon were moderately deep at 62 percent, and deep at 38 percent of the observation points. Based on sixteen measurements made with the EM38DD meter operating in the vertical dipole orientation and equation [4], the depths to the 2C horizon were shallow at 6 percent, moderately deep at 56 percent, and deep at 38 percent of the observation points.

Figure 14 shows the spatial distribution of depths to medium textured materials as measured with a soil auger (left-hand plot) and predicted with the GEM300 sensor (center plot) and the EM38DD meter (right-hand plot). In each plot the contour interval is 0.25 m. The location of each observation point is shown in each figure. With the exception of the northwest corner of the survey area, spatial patterns are remarkably similar for all instruments. At three observation points, differences of 0.03 to 0.1 m profoundly influenced the spatial patterns shown in the plot of the measured data. These differences caused the noted exception to the spatial patterns in the plots of the measured and interpreted data.

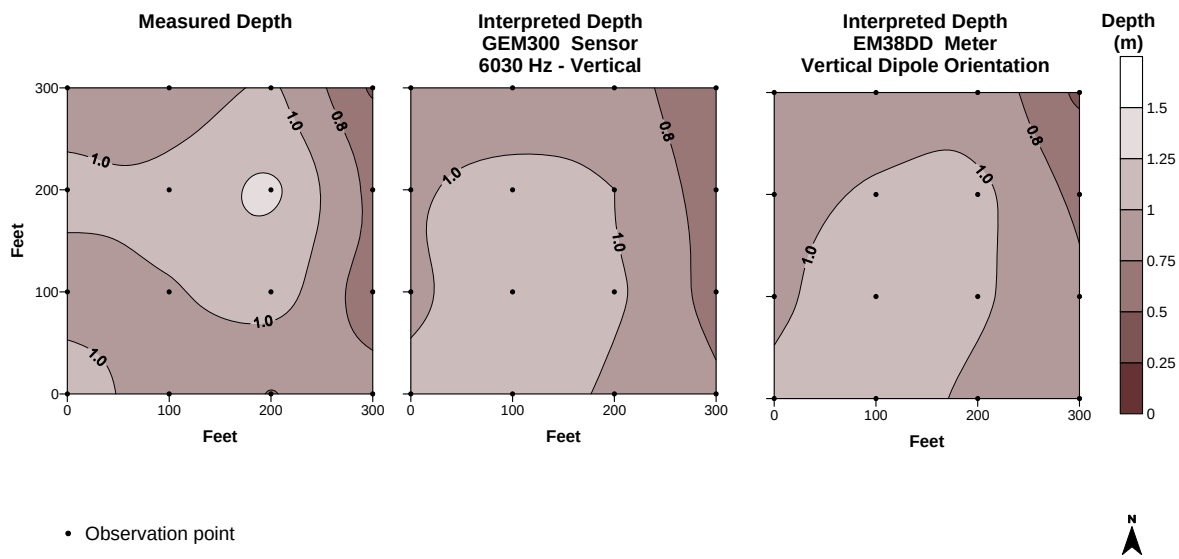

Figure 14. Measured and interpreted depths to medium textured materials. Interpretations based on station-to-station EMI measurements.

Most EMI instruments can be operated in the continuous mode and provide a large number of observations and more complete coverage of sites. Measurements from EMI instruments can be geo-referenced with GPS data eliminating the need for grids and providing the soil scientist with greater autonomy and mobility while eliminating the often-excessive time that is required to construct grids across units of management.

Additional surveys were completed across the site to demonstrate the expanding capacities of EMI systems. Data were collected in the continuous mode with the Geonics EM38Dpro Data Logging System. The EM38DD meter was carried at a height of about 6 cm above the ground surface. Walking at a fairly uniform pace along parallel grid lines, in a back and forth pattern across the field completed the EMI survey. Both EMI and GPS data were recorded at a rate

of one observation per second. Four traverses were conducted across the field (right-hand plot in Figure 15). This resulted in 267 observations.

When operated in the continuous mode, the GEM300 sensor cannot be rotated to record measurements in both dipole orientations. As a consequence, two separate surveys were required with the GEM300 sensor. Two surveys (one in the horizontal and one in the vertical dipole orientation) were conducted along the four north-south trending grid lines. The EMI survey was completed by walking at a uniform pace along each of the four grid lines. Surveys were completed with the GEM300 sensor held at hip height with its long axis parallel to the direction of traverse. EMI measurements were recorded at a rate of one observation per second. The coordinates of all observations collected with the GEM300 sensor were processed and adjusted by the MAGMAP96 software program developed by Geometrics. [2] This resulted in 297 and 289 observations recorded in the vertical and horizontal dipole orientations respectively.

Based on 289 measurements made with the GEM300 sensor operating in the continuous mode, at a frequency of 6030 Hz and in the vertical dipole orientation, and equation [3], the depths to medium textured deposits were shallow at 3 percent, moderately deep at 65 percent, deep at 31 percent, and very deep (>1.5 m) at 1 percent of the observation points. Based on 267 measurements made with the EM38DD meter operating in the continuous mode and in the vertical dipole orientation, and equation [3], the depths to medium textured deposits were moderately deep at 43 percent, and deep at 57 percent of the observation points. Though the spatial patterns of the depths to medium-textured soil materials obtained with the GEM300 sensor and the EM38DD meter are similar (see figure 15) and acceptable, the difference in depth classes is at first alarming. However a closer look at the data sets is settling. Based on 267 EM38DD observations, the average depth to medium-textured soil materials was 0.98 m with a range of 0.59 to 1.24 m. One half of the observations had measured depths between 0.89 and 1.10 m. Similarly, based on 289 GEM300 observations, the average depth to medium-textured soil materials was 0.92 m with a range of 0.42 to 2.32 m. One half of the observations had measured depths between 0.83 and 1.03 m. The data sets are spatially and statistically similar. Differences in the composition of soils based on soil depth classes reflect the placement of the "taxonomic chops".

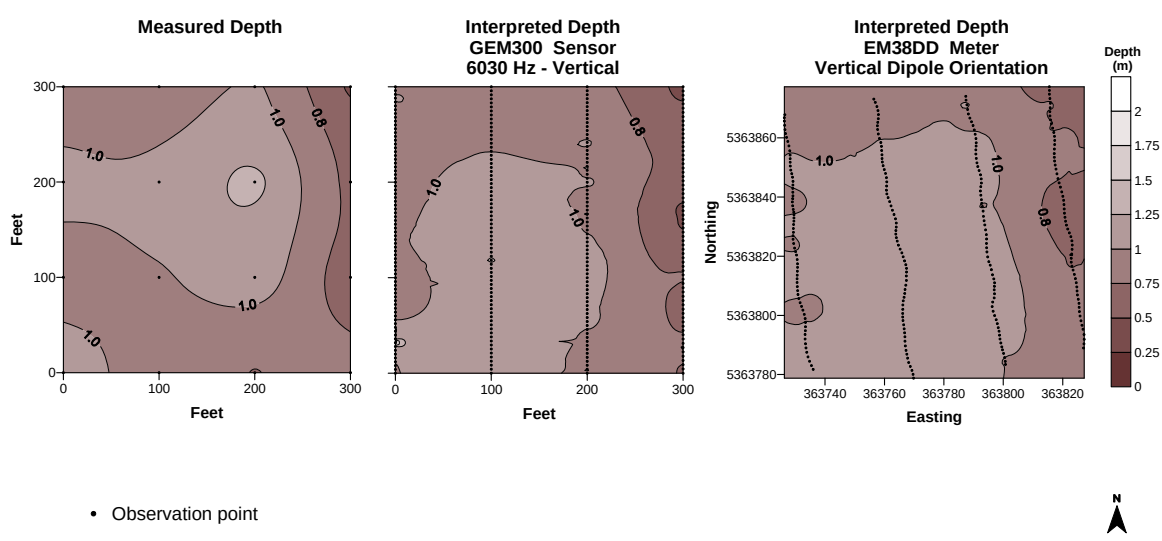

Figure 15. Measured and interpreted depths to medium textured materials. Interpretations based on continuous EMI measurements.

Reference:

Beres, M. and F. P. Haeni. 1991. Application of ground-penetrating radar methods in hydrogeologic studies. Ground Water 29(3): 375-386.

Bohling, G. C., M. P. Anderson, C. R. Bentley. 1989. Use of ground penetrating radar to define recharge areas in the Central Sand Plain. Technical Completion Report G1458-03. Geology and Geophysics Department, University of Wisconsin-Madison. 62 pp.

Cook, P. G. and G. R. Walker. 1992. Depth profiles of electrical conductivity from linear combinations of electromagnetic induction measurements. Soil Sci. Soc. Am. J. 56:1015-1022.

DesLauriers, L.L. 1990. Soil Survey of McHenry County, North Dakota. USDA-Soil Conservation Service. U.S. Government Printing Office, Washington, DC.

Doolittle, J. A. 1987. Using ground-penetrating radar to increase the quality and efficiency of soil surveys. pp. 11-32. In: Reybold, W. U. and G. W. Peterson (eds.) Soil Survey Techniques, Soil Science Society of America. Special Publication No. 20. p. 98

Doolittle, J. A. and M. E. Collins. 1995. Use of soil information to determine application of ground-penetrating radar. Journal of Applied Geophysics, 33:101-108.

Doolittle, J. A., and M. E. Collins. 1998. A comparison of EM induction and GPR methods in areas of karst. Geoderma 85:83-102.

Doolittle, J. A., B. J. Jenkinson, D. P. Franzmeier, and W. Lynn. 2000. Improved Radar Interpretations of Water Table Depths and Groundwater Flow patterns Using Predictive Equations. 488-495 pp. IN: (Noon, D. ed.) Proceedings Eight International Conference on Ground-Penetrating Radar. May 23 to 26, 2000, Goldcoast, Queenland, Australia. The University of Queensland.

Doolittle, J. A., F. E. Minzenmayer, S. W. Waltman, and E. C. Benham. 2002. Ground-penetrating radar soil suitability map of the conterminous United States. 7-12 pp. IN: Koppenjan, S. K., and L. Hua (eds). Ninth International Conference on Ground-Penetrating Radar. Proceedings of SPIE Volume 4158. 30 April to 2 May 2002. Santa Barbara, CA.

Doolittle, J., R. Murphy, G. Parks, and J. Warner. 1996. Electromagnetic induction investigations of a soil delineation in Reno County, Kansas. Soil Survey Horizons 37:11-20.

Edland, Lawrence. 1999. Soil survey of Ransom County, North Dakota. Interim Rpt. USDA-NRCS, Bismarck, ND.

Geonics Limited. 2000. EM38DD ground conductivity meter: Dual dipole version operating manual. Geonics Ltd., Mississauga, Ontario.

Geophysical Survey Systems, Inc, 2001a. RADAN for Windows NT; User's Manual - Condensed. Manual MN43-132 Rev C. Geophysical Survey Systems, Inc., North Salem, New Hampshire.

Geophysical Survey Systems, Inc, 2001b. 3D QuickDraw for RADAN NT; User's Manual. Manual MN43-143 Rev B. Geophysical Survey Systems, Inc., North Salem, New Hampshire.

Grant, J. A. and P. H. Schultz. 1994. Erosion of ejecta at Meteor Crater: Constraints from ground penetrating radar. pp. 789-803 IN: Proceedings Fifth International Conference on Ground-Penetrating Radar. Kitchner, Ontario, Canada, June 12 – 14, 1994. Waterloo Centre for Groundwater Research and the Canadian Geotechnical Society. p. 1294.

Greenhouse, J. P., and D. D. Slaine. 1983. The use of reconnaissance electromagnetic methods to map contaminant migration. Ground Water Monitoring Review 3(2): 47-59.

Hopkins, D. G., and M. D. Sweeney. 1987. Soil survey of the organized irrigation districts of McHenry County, North Dakota.
North Dakota Agricultural Experiment Station and USDA Soil Conservation Service. Fargo, ND.

Iivari, T. A. and J. A. Doolittle. 1994. Computer simulations of depths to water table using ground-penetrating radar in topographically diverse terrains. p. 11-20. IN: Kovar, K. and J. Soveri (eds.). Groundwater Quality Management (Proceedings of GQM 93, International Association of Hydrological Sciences. Conference held at Tallinn, Estonia. September 1993. 485 pp.

Jaynes, D. B., T. S. Colvin, J. Ambuel. 1993. Soil type and crop yield determination from ground conductivity surveys. 1993 International Meeting of American Society of Agricultural Engineers. Paper No. 933552. ASAE, St. Joseph, MI. pp. 6.

Johnson, D. G. 1987. Use of ground-penetrating radar for determining depth to the water table on Cape Cod, Massachusetts. p. 541-554. IN: Proceeding of First National Outdoor Action Conference on Aquifer Restoration, Ground Water Monitoring and Geophysical Methods. May 18-21, 1987. Las Vegas, Nevada. National Water Well Association, Dublin, Ohio.

Junck, M. B., and H. M. Jol. 2000. Three-dimensional investigation of geomorphic environments using ground penetrating radar. 314-318 pp. IN: (Noon, D. ed.) Proceedings Eight International Conference on Ground-Penetrating Radar. May 23 to 26, 2000, Goldcoast, Queensland, Australia. The University of Queensland. 908 p.

Kachanoski, R. G., E. G. Gregorich, and I. J. Van Wesenbeeck. 1988. Estimating spatial variations of soil water content using noncontacting electromagnetic inductive methods. Can. J. Soil Sci. 68:715-722.

McNeill, J. D. 1980. Electrical Conductivity of soils and rocks. Technical Note TN-5. Geonics Ltd., Mississauga, Ontario. 22 p.

Morey, R. M. 1974. Continuous subsurface profiling by impulse radar. pp. 212-232. IN: Proceedings, ASCE Engineering Foundation Conference on Subsurface Exploration for Underground Excavations and Heavy Construction, held at Henniker, New Hampshire. Aug. 11-16, 1974.

Opdahl, D. D., W. J. Terry, and N. D. Prochnow. 1990. Soil Survey of Barnes County, North Dakota. USDA-Soil Conservation Service. U.S. Government Printing Office, Washington, DC.

Rhoades, J. D., P. A. Raats, and R. J. Prather. 1976. Effects of liquid-phase electrical conductivity, water content, and surface conductivity on bulk soil electrical conductivity. Soil Sci. Soc. Am. J. 40:651-655.

Richardson, J. L., L. P. Wilding, and R. B. Daniels. 1992. Recharge and discharge of groundwater in aquic conditions illustrated with flow analysis. Geoderma 53: 65-78.

Soil Survey Staff. 1993. Soil Survey Manual. US Department of Agriculture - Soil Conservation Service, Handbook No. 18, US Government Printing Office. Washington, DC, USA. p. 437.

Steenhuis, T. S., K. -J. S. Kung, and L. M. Cathles III. 1990. Finding layers in the soil. Ground-penetrating radar as a tool in studies of groundwater contamination. Engineering Cornell Quarterly (Autumn) p. 15-19.

Sudduth, K. A., N. R. Kitchen, D. H. Hughes, and S. T. Drummond. 1995. Electromagnetic induction sensing as an indicator of productivity on claypan soils. pp. 671-681. IN: Robert, P. C., R. H. Rust, and W. E. Larson (editors). Proceedings of Second International Conference on Precision Management for Agricultural Systems. Minneapolis, Minnesota. March 27-30, 1994. American Society of Agronomy, Madison, Wisconsin.

Taylor, K. R. and M. E. Baker. 1988. Use of ground-penetrating radar in defining glacial outwash aquifers. p. 70-98. IN: Proceeding of the FOCUS Conference on Eastern Regional Ground Water Issues, Stamford, Connecticut. September 27-29, 1988. National Water Well Association, Dublin, Ohio.

Violette, P. 1987. Surface geophysical techniques for aquifers and wellhead protection area delineation. Environmental Protection Agency, Office of Ground Water Protection, Washington, D.C., 49 pp.

Won, I. J., Dean A. Keiswetter, George R. A. Fields, and Lynn C. Sutton. 1996. GEM-2: A new multifrequency electromagnetic sensor. Journal of Environmental & Engineering Geophysics 1:129-137.